TẠP CHÍ KHOA HỌC ĐẠI HỌC TÂN TRÀO
ISSN: 2354 - 1431
http://tckh.daihoctantrao.edu.vn/

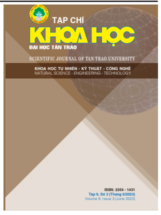

PATH LOSS MODEL IN INTELLIGENT RADIO ENVIRONMENT

Pham Van Ngoc, Do Thi Loan, Vu Thi Nguyet*
TNU - University of Information and Communication Technology
**Email address: dtloan@ictu.edu.vn*

DOI: 10.51453/2354-1431/2023/971

Article info

Received:11/12/2022

Revised:02/03/2023

Accepted: 16/5/2023

Keywords:

Reconfigurable intelligent surface, Intelligent reflecting surfaces, Beyond 5G, Pathloss model, Smart radio environment.

Abstract:

Smart reflective surface is a new technology that is being researched and deployed to develop wireless communication systems, as well as 5G, post-5G (B5G) and future 6G mobile networks. The surface contains reconfigurable electromagnetic metamaterial to direct the beam from the source to the desired receivers with maximum signal strength. The paper provides a pathloss and channel model in a smart surface-assisted communication system built based on physical-optical techniques and Snell's light reflection theorem. With mathematical expressions, it will provide researchers with a way to calculate, simulate, analyze, evaluate and calibrate communication channels to achieve optimal efficiency before deploying experimental fabrication. or for comparison with other information transfer enhancement technologies such as AF relay and amplifier, MIMO beamforming, and BackCom backscatter communication.

TẠP CHÍ KHOA HỌC ĐẠI HỌC TÂN TRÀO
ISSN: 2354 - 1431
http://tckh.daihoctantrao.edu.vn/

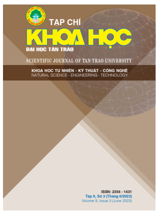

MÔ HÌNH SUY HAO ĐƯỜNG TRUYỀN TRONG MÔI TRƯỜNG VÔ TUYẾN THÔNG MINH

Phạm Văn Ngọc, Đỗ Thị Loan, Vũ Thị Nguyệt*
Trường Đại học Công nghệ Thông tin và Truyền thông - ĐH Thái Nguyên
Địa chỉ email: dtloan@ictu.edu.vn

DOI: 10.51453/2354-1431/2023/971

Thông tin bài viết

Ngày nhận bài: 11/12/2022
Ngày sửa bài: 02/03/2023
Ngày duyệt đăng: 16/5/2023

Từ khóa:

Bề mặt thông minh có thể cấu hình lại, Bề mặt phản xạ thông minh, Sau 5G, Mô hình pathloss, Môi trường vô tuyến thông minh.

Tóm tắt

Bề mặt phản xạ thông minh là một công nghệ mới đang được nghiên cứu, triển khai để phát triển các hệ thống truyền thông không dây, cũng như các mạng di động 5G, sau 5G (B5G) và mạng tương lai 6G. Bề mặt chứa siêu vật liệu điện từ có thể tái cấu hình để hướng chùm sóng từ nguồn phát tới các bộ thu mong muốn với cường độ tín hiệu tối đa. Bài báo cung cấp một mô hình pathloss và kênh dẫn trong hệ thống thông tin liên lạc có sự hỗ trợ của bề mặt thông minh được xây dựng dựa trên kỹ thuật quang học vật lý và định luận phản xạ ánh sáng của Snell. Với các biểu thức toán học sẽ cung cấp cho các nhà nghiên cứu một phương án tính toán, mô phỏng, phân tích, đánh giá và hiệu chỉnh các kênh truyền thông nhằm đạt được hiệu quả tối ưu trước khi triển khai chế tạo thực nghiệm hoặc để so sánh với các công nghệ tăng cường truyền tải thông tin khác như bộ khuếch đại và chuyển tiếp AF, định dạng chùm MIMO và truyền thông tán xạ ngược BackCom.

1. Introduction

A basic wireless communication system consists of a transmitter that carries information to a receiver through an uncontrolled electromagnetic wave propagation environment. The 5G network technology, also known as B5G, is moving towards the future 6G network and requires the implementation of support technologies, called smart reflective surfaces, that can reconfigure the transmission environment in real-time [1]-[4] These surfaces are also known as software-controlled meta-surfaces [2]-[4], reconfigurable intelligent surfaces [5],[6], etc. In an intelligent radio environment [7], incoming waves can be controlled for reflection, diffraction, scattering and refraction in desired directions.

The newly designed reconfigurable surfaces are in basic form [8], without a standardized propagation model. Currently, there are two proposed path loss models: based on passive reflective arrays [9],[10], where the antennas of the elements can be controlled to scatter the wave backward or phase shift the signal to the receiver, and based on meta-surfaces [5], a two-dimensional flat shape using artificial electromagnetic materials.

This paper provides a path loss model for intelligent reflective surfaces to allow for computing, analyzing, and simulating information, thereby evaluating the performance of this technology and comparing it with other technical support methods.

2. Smart surfaces designed based on passive reflective arrays

Consider a wave beam incident on a finite-size passive reflective array (a x b) with negligible thickness lying in the plane (ex, ey). A transmitting source is located at a sufficient distance from the surface (compared to a and b) and the wave number is k= 2π/λ (wavelength λ) with an incident angle of θi ∈[0; π/2]

The smart surface is oriented so that the Poynting vector (the product of the electric field intensity and magnetic field intensity that describes the energy of the electromagnetic wave in a unit time on a unit area) enters with θi = 0 at the center of the reflective array and can be analyzed in general at arbitrary incident angles. Based on the plane wave approximation, the wave from the transmitter would reach any point on the surface at a distance of di. However, in reality, the wave is spherical and at the edges of the surface, the transmitted distance is given by: $\sqrt{d_i^2+\frac{b^2}{4}}$.

In that case, the phase difference is:

$$k\left(\sqrt{d_i^2+\frac{b^2}{4}}-d_i\right)\approx\frac{\pi}{4}\frac{b^2}{\lambda d_i} \tag{1}$$

The incident plane wave has an electric and magnetic field distribution of:

$$\mathbf{E}_i = E_i e^{-jk\left(\sin\left(\theta_i\right)y-\cos\left(\theta_i\right)z\right)}\boldsymbol{e}_x \tag{2}$$

$$\mathbf{H}_i = -\frac{E_i}{\eta}\left(\cos\left(\theta_i\right)e_y+\sin\left(\theta_i\right)\boldsymbol{e}_z\right)e^{-jk\left(\sin\left(\theta_i\right)y-\cos\left(\theta_i\right)z\right)} \tag{3}$$

Where η is the characteristic impedance of the medium. The magnetic field E generates motion of electrons in the reflective array. The electrons move in the ex direction, but not in the ey direction (because E is orthogonal to ey) and not in the ez direction because the surface has negligible thickness. The motion of the electrons causes electromagnetic radiation, creating scattered waves. The squared amplitude of the scattered field in the ey, ez plane at an arbitrary observation angle θs ∈[0; π/2], measured along ez at a distance of r, $r\geq\frac{2max\left(a^2,b^2\right)}{\lambda}$ is:

$$S(r,\theta_s) = \left(\frac{ab}{\lambda}\right)^2\frac{E_i^2}{r^2}cos\ ^2(\theta_i)\Bigg(\frac{sin\Big(\frac{\pi b}{\lambda}(sin(\theta_s)-sin(}{\frac{\pi b}{\lambda}(sin(\theta_s)-sin(\theta_i}\quad 4)$$

This result is based on standard physical optics techniques (ignoring edge effects) [11] According to Snell's law of light reflection, S(r,θs) reaches a maximum value at the special direction where θs = θi. The maximum viewing angle increases as the size of the surface increases. The expression S(r,θs) shows that the scattered field decreases as θs moves away from θi. The 3dB beamwidth is twice the deviation |θs - θi| required to make the second term in parentheses equal to 1/2. Using the Taylor expansion cos(x) = 1 + O(x2) and standard trigonometric identities, we have:

$$\begin{aligned}\sin\left(\theta_s\right)-\sin\left(\theta_i\right)&=\sin\left(\theta_i+\theta_s-\theta_i\right)-\sin\left(\theta_i\right)=\sin\left(\theta_i\right)\cos\left(\theta_s-\theta_i\right)+\cos\left(\theta_i\right)\sin\left(\theta_s-\theta_i\right)-\sin\left(\theta_i\right)\\&=\cos\left(\theta_i\right)\left(\theta_s-\theta_i\right)+O\left(\left(\theta_s-\theta_i\right)^2\right)\end{aligned} \tag{5}$$

Using Taylor series expansion $\frac{\sin\left(x\right)}{x}=1-\frac{x^2}{6}+O\left(x^3\right)$ and $\left(\frac{\sin\left(x\right)}{x}\right)^2=1-\frac{x^2}{3}+O\left(x^3\right)$, we obtain the second-order approximation:

$$S\left(r,\theta_s\right)=\left(\frac{ab}{\lambda}\right)^2\frac{E_i^2}{r^2}\cos^2\left(\theta_i\right)\left(1-\frac{\pi^2b^2}{\lambda^2}\frac{\cos^2\left(\theta_i\right)\left(\theta_s-\theta_i\right)^2}{3}\right)+O\left(\left(\theta_s-\theta_i\right)^3\right) \tag{6}$$

Therefore, the 3dB beamwidth is approximately twice the deviation |θs - θi| required to create:

$$\frac{\pi^2 b^2}{\lambda^2}\frac{\cos^2(\theta_i)(\theta_s-\theta_i)^2}{3}=\frac{1}{2} \qquad (7)$$

$$|\theta_s-\theta_i|<\sqrt{\frac{1}{2}\frac{3\lambda^2}{\pi^2 b^2\cos^2(\theta_i)}}=\sqrt{\frac{3}{2}}\frac{\lambda}{\pi b\cos(\theta_i)} \qquad (8)$$

This inequality shows that the 3dB beamwidth is inversely proportional to the width b. The beamwidth is also proportional to the wavelength λ, so a fixed-size array can provide beamwidths in visible spectra (near-perfect reflection), but wider beamwidths by 4-5 orders of magnitude in typical radio spectra. The array acts as a diffraction or scattering field whose 3dB beamwidth is inversely proportional to b. If the reflective surface is regarded as an antenna, the beamwidth is inversely proportional to the antenna aperture.

For the squared intensity S(r,θs) with θi = 30◦, when a and b are smaller than or equal to the wavelength, the scattered field is almost equally strong at all observation angles. When the reflective surface is significantly larger than λ, the beamwidth is narrow. The 3dB beamwidth is ≈5.7◦ for a=b=10λ and ≈5.2◦.

A receiving antenna with an effective size of λ/v×λ/v, placed at an angle θs to the reflective array, picks up a signal power: $S(r,\theta_s)\left(\frac{\lambda}{v}\right)^2$. The antenna sees the reflective surface at a viewing angle of $\frac{\lambda}{vr}$ radians. If $\frac{\lambda}{vr} \ll \frac{\lambda}{b\cos(\theta_i)}$, that is approximately constant, $r \gg b/v$ the electric field intensity is approximately independent of the antenna.

Since $E_i^2 \propto 1/d_i^2$, the received power is proportional to (ab)2=(dir)2 where , and the constant of proportionality depends on the wavelength and angle. If θs = θi, The received power increases with a and b, as more energy is brought into the array and then radiated in a narrower beam. Even if the beamwidth is small compared to λ = r, most of the energy of the scattered field is still ignored by the antenna aperture. This is the reason why the received power in (8) is proportional to 1/r2. When a and b increase without constraint, the flat wave approximation of the incident field is eventually broken and the results in this section become inaccurate.

Because the reflective array has a finite size, multiple adjacent panels can be deployed. If the spacing between them is large enough, coupling effects can be ignored. When the scattered field from these panels is received at a specific position, relative phase shifts will lead to constructive or destructive interference. Under ideal constructive interference, the squared field intensity from N panels is:

$$\left(N\sqrt{S(r,\theta_s)}\right)^2=N^2 S(r,\theta_s) \qquad (9)$$

Where Nab is the sum of the area of N panels. Therefore, whether the reflective array is composed of many small panels or a few large ones, the maximum received power is the same.

3. System Model of Intelligent Reflecting Surfaces

An intelligent reflecting surface is considered as a meta-surface. The objective is to achieve full reflection with the main beam directed towards the desired receiver location at an angle θr. Therefore, the surface must be designed to redirect the incident wave (Ei, Hi) and receive the ideal field distributions of the reflected/scattered wave::

$$\mathbf{E}_r=E_r e^{-jk(\sin(\theta_r)y+\cos(\theta_r)z)}e_x \qquad (10)$$

$$\mathbf{H}_r=-\frac{E_r}{\eta}\left(\sin(\theta_r)\boldsymbol{e}_z-\cos(\theta_r)\boldsymbol{e}_y\right)e^{-jk(\sin(\theta_r)y+\cos(\theta_r)z)} \qquad (11)$$

The approach is based on the design of metasurfaces following Snell's general reflection law [12] The required phase profile of the surface needed to transform the incident wave (Ei, Hi) into (Er, Hr) is obtained by adjusting the surface impedance. At z = 0, the superposition of the incident field and the reflected E field is [13]:

$$\mathbf{E}_t = E_i e^{-\mathrm{jk}\sin(\theta_i)y}\boldsymbol{e}_x + E_r e^{-\mathrm{jk}\sin(\theta_r)y}\boldsymbol{e}_x \tag{12}$$

Then, the desired phase of the reflection coefficient is:

$$\phi_r(y) = \angle\left(\frac{E_r e^{-jk\sin(\theta_r)y}}{E_i e^{-jk\sin(\theta_i)y}}\right) = -k\sin(\theta_r)y + k\sin(\theta_i)y \tag{13}$$

Differentiating it with respect to y, the gradient of the reflection coefficient following Snell's general law is obtained:

$$k\left(\sin(\theta_i) - \sin(\theta_r)\right) = \frac{d\phi_r(y)}{dy} \tag{14}$$

The relationship between θi, θr, and the local surface phase φr(y) is established. By varying the surface impedance, the φr(y) is obtained at each point on the reflection plane, and the desired output wave phase is achieved:

$$-k\sin(\theta_i)y + \phi_r(y) = -k\sin(\theta_r)y \tag{15}$$

In [14], the phase distribution is customized and quantized with a step size of λ = 5 to represent a finite number of phase shifters used. In [15], the surface is stepped with λ = 8. High-precision small elements require complex design and fabrication and difficult interconnection. On the other hand, if the elements are too large compared to λ, it will lead to a mismatch between the desired reflection angle and the reflection from the surface.

An intelligent reflecting surface needs to include many small elements to configure local phases to obtain the desired beam direction with an angle θr. The E field of the incident wave generates a surface current along the ex direction. This current is adjusted by changing the surface impedance in each element to obtain an approximate phase configuration according to Snell's law. This operation generates a scattered wave with a maximum amplitude directed towards θr instead of θi.

When using a surface to reflect signals in the direction of θr, the magnitude squared of the scattering field at an arbitrary observation angle $\theta_s \in \left[-\frac{\pi}{2}, \frac{\pi}{2}\right]$ at a distance $r \geq \frac{2\max(a^2, b^2)}{\lambda}$ is:

$$S_{\mathrm{IRS}}\left(r, \theta_s, E_i^2\right) = \left(\frac{ab}{\lambda}\right)^2 \frac{E_i^2\cos^2(\theta_i)}{r^2}\left(\frac{\sin\left(\frac{\pi b}{\lambda}\left(\sin(\theta_s) - \sin(\theta_r)\right)\right)}{\frac{\pi b}{\lambda}\left(\sin(\theta_s) - \sin(\theta_r)\right)}\right)^2 \tag{16}$$

The surface thickness insignificance provides an approximation of the surface current density at z = 0 [11]:

$$J_x = \frac{2E_i}{\eta}\cos(\theta_i)e^{-jk\sin(\theta_r)y'} \tag{17}$$

Assuming an ideal lossless surface, i.e $E_i^2\cos(\theta_i) = E_r^2\cos(\theta_r)$. Let Pt be the power supplied by the source and Gt be the antenna gain of the transmitter. The relation between Ei and Pt is:

$$\frac{E_i^2}{2\eta} = \frac{P_t G_t}{4\pi d_i^2} \tag{18}$$

The effective area of the receive antenna is $\frac{\lambda^2}{4\pi}G_r$, where Gr is the gain of the antenna. The received signal power Pr at a distance r in the direction of θs is:

$$P_r\left(P_t,d_i,r,\theta_s\right)=\frac{1}{2\eta}S_{\text{IRS}}\left(r,\theta_s,\frac{P_tG_t\eta}{2\pi d_i^2}\right)\left(\frac{\lambda^2}{4\pi}G_r\right) \tag{19}$$

When using an intelligent surface to reflect signals in the direction of θr, the path loss at a distance r has the expression:

$$\beta_{\text{IRS}}\left(r,d_i,\theta_s\right)=\frac{P_r\left(P_t,d_i,r,\theta_s\right)}{P_t}=\frac{G_tG_r}{(4\pi)^2}\left(\frac{ab}{d_ir}\right)^2\cos^2\left(\theta_i\right)\left(\frac{\sin\left(\frac{\pi b}{\lambda}\left(\sin\left(\theta_s\right)-\sin\left(\theta_r\right)\right)\right)}{\frac{\pi b}{\lambda}\left(\sin\left(\theta_s\right)-\sin\left(\theta_r\right)\right)}\right)^2 \tag{20}$$

For the ideal case where θs = θr, the path loss expression simplifies to:

$$\beta_{\text{IRS}}\left(r,d_i,\theta_r\right)=\frac{G_tG_r}{(4\pi)^2}\left(\frac{ab}{d_ir}\right)^2\cos^2\left(\theta_i\right) \tag{21}$$

The path loss expression only depends on the effective area of the intelligent surface when viewed from the transmitter. is a function of θs with different surface sizes and θr = 60°. The maximum level is achieved when θs = θr, and the main beamwidth narrows as the surface area increases. When the integer part is a subwavelength (≤ λ/ 2), the surface acts as a diffusely scattering array.

The smart reflective surface is modeled as an array of passive reflection elements, each with a size smaller than λ. Assume the intelligent surface comprises Na × Nb elements, each with a size of: $\frac{a}{N_a}\times\frac{b}{N_b}$, $\frac{a}{N_a},\frac{b}{N_b}\leq\lambda$. The path loss model between the transmitter and receiver through the nth surface element (assuming other elements are removed) is:

$$\beta_{\text{IRS}}^{s}\left(r,d_i,\theta_r\right)=\frac{G_tG_r}{(4\pi)^2}\left(\frac{ab}{N_aN_bd_ir}\right)^2\cos^2\left(\theta_i\right) \tag{22}$$

Note that $\beta_{\text{IRS}}^{s}\left(r,d_i,\theta_r\right)$ for all n since the assumption is identical for every element $r\geq\frac{2\max\left(a^2,b^2\right)}{\lambda}$. Let ϕ_n represent the local surface phase of the nth element. If it is chosen to achieve interference from all surface elements $N=N_aN_b$ at the receiver, the path loss between the transmitter and the receiver through the entire intelligent surface is:

$$\left(N\sqrt{\beta_{\text{IRS}}^{s}\left(r,d_i,\theta_r\right)}\right)^2=\beta_{\text{IRS}}\left(r,d_i,\theta_s\right) \tag{23}$$

Thus, the intelligent surface comprises an array of diffuse scattering elements (each with a size of λ) arranged in a phase sequence of their reflected signals at the receiver and hence achieves the desired reflection.

The physical setup of the intelligent surface-supported wireless communication system is considered to establish a line of sight (LoS) in which $\sqrt{\beta_{\text{sd}}}e^{j\phi_{\text{sd}}}$ is the direct channel between the source and the destination receiver. When considering the reflection path from the intelligent surface, the receiver receives the total received signal:

$$y=\left(\sqrt{\beta^{s}_{\mathrm{IRS}}}\mathbf{h}^{\mathrm{T}}_{\mathrm{sr}}\mathbf{\Phi}\mathbf{h}_{\mathrm{rd}}+\sqrt{\beta_{\mathrm{sd}}}e^{j\phi_{\mathrm{sd}}}\right)x+w \quad (24)$$

where $\mathbf{h}_{\mathrm{sr}}=\left[e^{j\psi_1^{\mathrm{sr}}},\ldots,e^{j\psi_n^{\mathrm{sr}}},\ldots,e^{j\psi_N^{\mathrm{sr}}}\right]^{\mathrm{T}}$ and $\mathbf{h}_{\mathrm{rd}}=\left[e^{j\psi_1^{\mathrm{rd}}},\ldots,e^{j\psi_n^{\mathrm{rd}}},\ldots,\right]^{\mathrm{T}}$ are the normalized LoS channels between the source with the surface and the surface with the receiver, respectively. The signal x with power is noise P_t, $w\sim\mathrm{N}_{\mathrm{C}}\left(0,\sigma^2\right)$ The signal x with power is noise, and the local phases of each element stacked in form a diagonal matrix $\mathbf{\Phi}=\mathrm{diag}\left(e^{j\phi_1},\ldots,e^{j\phi_n},\ldots,e^{j\phi_N}\right)$. Therefore:

$$y=\sqrt{\beta^{s}_{\mathrm{IRS}}}\sum_{n=1}^{N}e^{j\left(\psi_n^{\mathrm{sr}}+\psi_n^{\mathrm{rd}}+\phi_n\right)}x+\sqrt{\beta_{\mathrm{sd}}}e^{j\phi_{\mathrm{sd}}}x+w \quad (25)$$

The intelligent surface can be chosen such that Φ maximizes the received signal power [9] If is chosen $\phi_n=\phi_{\mathrm{sd}}-\psi_n^{\mathrm{sr}}-\psi_n^{\mathrm{rd}}$ to align the phase of all signals, then:

$$y=\left(N\sqrt{\beta^{s}_{\mathrm{IRS}}}+\sqrt{\beta_{\mathrm{sd}}}\right)e^{j\phi_{\mathrm{sd}}}x+w \quad (26)$$

The signal-to-noise ratio (SNR) is:

$$\mathrm{SNR}=\frac{\left(N\sqrt{\beta^{s}_{\mathrm{IRS}}}+\sqrt{\beta_{\mathrm{sd}}}\right)^2P_t}{\sigma^2}=\frac{\left(\sqrt{\beta_{\mathrm{IRS}}}+\sqrt{\beta_{\mathrm{sd}}}\right)^2P_t}{\sigma^2} \quad (27)$$

Therefore, local phase shifts are considered equivalent to the customizable Snell's law shifts, provided they are additionally phase-aligned with the LoS path. If the intelligent surface is used for reflection in the desired direction, the total path of the wave with the phases of the surface elements is adjusted. Then, choose a common ϕ_{IRS} for all elements ϕ_{sd} to make equal:

$$y=\sqrt{\beta_{\mathrm{IRS}}}e^{j\phi_{\mathrm{IRS}}}x+\sqrt{\beta_{\mathrm{sd}}}e^{j\phi_{\mathrm{sd}}}x+w \quad (28)$$

4. Conclusion

Using physical optics techniques, we have obtained the formula to determine the path loss for an intelligent reflecting surface configured to control wave propagation in the desired direction, transforming the random wireless transmission process into an intelligent wireless environment. Even when the incoming signal is a plane wave, the reflected signal is a beam with a width inversely proportional to the size of the array surface. The received signal power is proportional to the square of the reflection array and 1/(dir)2, (di is the distance between the transmitter and the reflection array, r is the distance between the reflection array and the receiver).

An intelligent reflection array consisting of N subwavelength-sized elements scatter the signal with a unique phase shift to achieve a coherent beam in the desired direction. The ideal phase shift generates a single beam that is directed by the generalized Snell's law. However, if multiple beams are to be formed, the phase shift must be optimized explicitly to achieve the coherent superposition of all beams.

With the path loss model and mathematical expressions for wireless communication system transmission paths using the supported intelligent surface, researchers can refer to them to simulate, analyze, evaluate, and optimize communication channels before implementing experimental manufacturing or comparing with other enhanced transmission technologies such as Amplify and Forward (AF) relay and amplification, massive MIMO beamforming, and Backscatter Communications reverse transmission scattering communication.

The use of intelligent surfaces in wireless communication systems has the potential to greatly improve communication efficiency and quality, especially in challenging environments such as densely populated areas or underground tunnels. The study of intelligent surfaces and their path loss models is an important step toward realizing the full potential of this emerging technology.

References

[1] M. Patzold, "It's time to go big with 5G mobile radio," *IEEE Vehicular Technology Magazine,* vol. 13, no. 4, pp. 4-10, 2018.

[2] W. Saad, M. Bennis, and M. Chen, "A vision of 6G wireless systems: Applications, trends, technologies, and open research problems," *in IEEE Network*, vol. 34, no. 3, pp. 134 - 142, Oct. 2019.

[3] X. Cao, L. Liu, Y. Cheng, and X. S. Shen, "Towards energy-efficient wireless networking in the big data era: A survey," *IEEE Commun. Surv. Tut*., vol. 20, no. 1, pp. 303-332, Firstquarter 2018.

[4] M. R. Akdeniz et al., "Millimeter wave channel modeling and cellular capacity evaluation," *IEEE J. Sel. Areas Commun*., vol. 32, no. 6, pp. 1164-1179, Jun. 2014.

[5] Q. Wu and R. Zhang, "Towards smart and reconfigurable environment: Intelligent reflecting surface aided wireless network*," IEEE Commun. Mag*., vol. 58, no. 1, pp. 106-112, Jan. 2020.

[6] M. D. Renzo et al., "Smart radio environments empowered by reconfigurable AI meta-surfaces: An idea whose time has come," *EURASIP J. Wireless Commun. Netw*., vol. 2019, May 2019, Art. no. 129.

[7] E. Basar, M. Di Renzo, J. de Rosny, M. Debbah, M.-S. Alouini, and R. Zhang, "Wireless communications through reconfigurable intelligent surfaces," in *IEEE Access*, vol. 7, pp. 116753 - 116773, Aug. 2019.

[8] E. Basar, "Transmission through large intelligent surfaces: A new frontier in wireless communications," *European Conference on Networks and Communications (EuCNC*), 2019.

[9] Z.-Q. He and X. Yuan, "Cascaded channel estimation for large intelligent metasurface assisted massive MIMO," in *IEEE Wireless Communications Letters*, vol. 9, pp. 210 - 214, Oct. 2019.

[10] X. Tan, Z. Sun, D. Koutsonikolas, and J. M. Jornet, "Enabling indoor mobile millimeter-wave networks based on smart reflect-arrays," *IEEE Conference on Computer Communications (INFOCOM)*, 2018, pp. 270-278.

[11] T. Ulversoy, "Software defined radio: Challenges and opportunities," *IEEE Communications Surveys & Tutorials,* vol. 12, no. 4, pp. 531-550, 2010.

[12] D. Mishra and H. Johansson, "Channel estimation and low-complexity beamforming design for passive intelligent surface assisted MISO wireless energy transfer," in *IEEE International Conference on Acoustics, Speech and Signal Processing (ICASSP), 2019*, pp. 4659-4663.

[13] L. Subrt and P. Pechac, "Controlling propagation environments using intelligent walls," *proc. European Conf. Antennas Propag. (EUCAP),* Mar. 2012, pp. 26-30.

[14] M. Najafi and R. Schober, "Intelligent reflecting surfaces for free space optical communications," proc. *IEEE GLOBECOM*, Dec. 2019, pp. 1-7.

[15] Z. Li et al., "Towards programming the radio environment with large arrays of inexpensive antennas," in *Proc. USENIX Symp. Netw. Syst. Design Implement*., Feb. 2019, pp. 285-299.